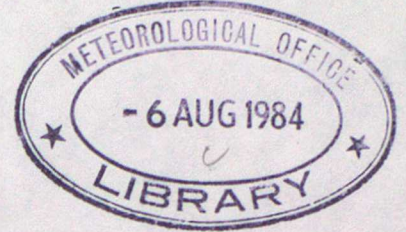


Lib

143887

MET.O.14

METEOROLOGICAL OFFICE
BOUNDARY LAYER RESEARCH BRANCH
TURBULENCE & DIFFUSION NOTE



TDN No 158

A REVIEW OF THE PROFILE METHOD OF ESTIMATING
SURFACE TURBULENT FLUXES

by

Wang Jiemin*

The Institute of Plateau Atmospheric Physics
Chinese Academy of Sciences
Lanzhou, China

*This work was carried out at the Boundary Layer Research Branch,
Meteorological Office, UK.

METEOROLOGICAL OFFICE

JUL 1984

M. O. 14

Please note: Permission to quote from this unpublished note should be
obtained from the Head of Met.O.14; Bracknell, Berks, U.K.

A REVIEW OF THE PROFILE METHOD OF ESTIMATING
SURFACE TURBULENT FLUXES

by

Wang Jiemin*

The Institute of Plateau Atmospheric Physics
Chinese Academy of Sciences
Lanzhou, China

*This work was carried out at the Boundary Layer Research Branch,
Meteorological Office, UK.

A review of the profile method of estimating surface turbulence fluxes

1. Introduction

The importance of specifying the stability of the surface layer of the atmospheric boundary layer in air pollution dispersion analysis is widely recognised. The surface friction velocity, U_* , and the surface sensible heat flux, H , are the two basic stability determinants. Direct evaluation of U_* and H can only be obtained from extensive and difficult turbulence measurements, the equipment used being either very expensive (e.g. sonic anemometer) or too fragile to be used in routine work (e.g. hot-wire anemometer). The profile method, which has been fully developed in the past 10-15 years, has proved to be a reliable method for estimating surface fluxes, and hence the stability parameter. The instruments used are readily available and do not require daily calibration and maintenance. Since wind at only one level and temperature at two levels (or one vertical temperature difference) may suffice for the calculation, this method is very appealing for use in routine meteorological work.

2. Generalized flux-gradient relationships

The profile method for the estimation of surface turbulent fluxes is based on Monin-Obukhov similarity theory for the surface layer. According to the similarity theory, under an assumption of stationary and horizontally homogeneous conditions, vertical gradients of any conservative quantity are functions of height, z , and $\zeta = Z/L$ only, where the Monin-Obukhov length, L , is defined by the usual notation

$$L = - \frac{\bar{\theta}}{g} \frac{\rho C_p U_*^3}{k H} \quad (1)$$

The generalized flux-gradient relationships, for wind, U , and potential temperature, θ , are expressed in the form

$$\frac{\partial U}{\partial Z} = \frac{U_*}{kZ} \phi_m(\zeta) \quad (2)$$

$$\frac{\partial \theta}{\partial z} = \frac{-\theta_*}{kZ} \phi_h(\zeta) \quad (3)$$

where θ_* is a temperature scale defined by

$$\theta_* = H/\rho C_p$$

A corresponding relationship is adopted for the profile of specific humidity with the assumption that $\phi_h(\zeta)$ is the appropriate similarity function.

The similarity functions ϕ_m and ϕ_h must be empirically determined from analysis of surface layer observations. Almost all authors have turned to the following general forms for ϕ ,

Under unstable conditions ($\zeta < 0$)

$$\phi_m = (1 - \gamma_m \zeta)^{-1/4} \quad (4)$$

$$\phi_h = \alpha(1-\gamma_h\zeta)^{-1/2} \quad (5)$$

Under stable conditions ($\zeta > 0$)

$$\phi_m = 1+\beta\zeta \quad (6)$$

$$\phi_h = \alpha+\beta\zeta \quad (7)$$

To determine the parameters α , β and γ requires a series of accurate measurements of temperature difference, wind speed, as well as the direct measurements of fluxes concerned. There are at present two widely used sets of parameterization

1. $\gamma_m = 15$, $\gamma_h = 9$, $\alpha = 0.74$, $\beta = 4.7$ (Businger et al, 1971)

2. $\gamma_m = 16$, $\gamma_h = 16$, $\alpha = 1.0$, $\beta = 5.0$
(Dyer and Hicks, 1970; Hicks, 1976; Dyer, 1974)

Caution: in Businger's parameterization the von Karman constant k is taken to be 0.35 instead of the more commonly used 0.40.

Fig. 1 shows the similarity functions ϕ_m and ϕ_h (divided by k) as a function of ζ for both Businger et al and Dyer and Hicks parameterizations. The difference between the two schemes is very small. We have used both schemes to process the Cardington 1983 profile data (Wang, 1984). The resultant differences in fluxes are less than 5%.

3. Integrated profile relationships

Direct use of flux-gradient relationships requires wind and temperature gradients, $\Delta U/\Delta z$ and $\Delta \theta/\Delta z$, at several closely separated heights. In practice, it is convenient to use the integrated profiles to evaluate the fluxes. Integrating (2) and (3) between two heights Z_1 and Z_2 , one obtains

$$U(Z_2) - U(Z_1) = \frac{U_*}{k} \psi_m \quad (8)$$

$$\theta(Z_2) - \theta(Z_1) = \frac{-\theta_*}{k} \psi_h \quad (9)$$

There are two ways of expressing the exact results of integration.

a. e.g. Nickerson and Smiley, 1975.

Unstable case

$$\psi_m = \ln \left(\frac{X_2-1}{X_2+1} \frac{X_1+1}{X_1-1} \right) + 2 (\tan^{-1} X_2 - \tan^{-1} X_1) \quad (10)$$

$$\psi_h = \alpha \ln \left(\frac{Y_2-1}{Y_2+1} \frac{Y_1+1}{Y_1-1} \right) \quad (11)$$

Stable case

$$\psi_m = \ln \frac{Z_2}{Z_1} + \frac{\beta}{L} (Z_2 - Z_1) \quad (12)$$

$$\psi_h = \alpha \ln \frac{Z_2}{Z_1} + \frac{\beta}{L} (Z_2 - Z_1) \quad (13)$$

b. e.g. Benoit, 1977

Unstable case

$$\psi_m = \ln \frac{Z_2}{Z_1} + \ln \left[\frac{(X_1^2+1)(X_1+1)^2}{(X_2^2+1)(X_2+1)^2} \right] + 2 (\tan^{-1} X_2 - \tan^{-1} X_1) \quad (14)$$

$$\psi_h = \alpha \left[\ln \frac{Z_2}{Z_1} + 2 \ln \left(\frac{Y_1+1}{Y_2+1} \right) \right] \quad (15)$$

Stable case

Same as (12), (13)

where

$$X_1 = (1 - \gamma_m Z_1/L)^{1/4}$$

$$X_2 = (1 - \gamma_m Z_2/L)^{1/4}$$

$$Y_1 = (1 - \gamma_h Z_1/L)^{1/2}$$

$$Y_2 = (1 - \gamma_h Z_2/L)^{1/2}$$

In fact, expressions a. and b. are fully equivalent. But for the numerical evaluation of U_* , θ_* , and hence the fluxes, the latter formulae have the advantage that they do not suffer from uncertainties when $|L|$ becomes very large, i.e. tends to neutral stratification, on the unstable side. The former relationships have this problem. It is due to the appearance of 0/0 type fraction in equations (10) and (11) as $|L| \rightarrow \infty$, X and $Y \rightarrow 1$.

In the usual profile observations the wind and temperature are not measured at the same heights. So in eqs. (10) - (15) Z_1 , Z_2 (and X, Y) should be changed accordingly: For ψ_m , $Z_1 = Z_{u1}$, $Z_2 = Z_{u2}$; for ψ_h , $Z_1 = Z_{T1}$, $Z_2 = Z_{T2}$.

Fig. 2 shows the behaviour of ψ_m as a function of height (Z) under different stabilities ($L = -0.001$ to ∞ , 0.1 to ∞), assuming $Z_1 = Z_0 = 0.01$ m. Z_0 is the roughness length.

In Fig. 2, $\psi_m = (k/U_*) \Delta U = (k/U_*) U(z)$. The straight line ($L = \infty$) on the semi-logarithmic graph represents the neutral case wind profile. It can be seen, in the case of unstable conditions ($L < 0$) that the wind speed increases with height initially slower than logarithmic, approaching finally a constant value. In the case of a stable stratification ($L > 0$), the increase of U is initially faster than logarithmic, then becoming almost linear. But we must bear in mind the limit of the similarity functions. Strictly speaking, the similarity theory is valid only in the surface layer, and both the

Businger et al and Dyer and Hicks formulae are applicable only within a limited range of stabilities (Businger et al: $Z/L = -2.0$ to 1.5 , Dyer and Hicks: -1.0 to 0.5).

4. The calculation of surface fluxes from profile data

To obtain the fluxes from a set of good wind and temperature profiles, the complete set of equations to be solved becomes:-

$$U(Z_{u2}) - U(Z_{u1}) = \frac{U_*}{k} \psi_m \quad (16a)$$

$$\theta(Z_{T2}) - \theta(Z_{T1}) = \frac{-\theta_*}{k} \psi_h \quad (16b)$$

$$L = - \frac{\bar{\theta}}{g} \frac{U_*^2}{k\theta_*} \quad (16c)$$

$$H = \rho C_p U_* \theta_*$$

From (16a) to (16c)

$$L = \frac{\bar{\theta}}{g} \frac{(\Delta U)^2}{\Delta \theta} \frac{\psi_h}{\psi_m^2} \quad (17)$$

where $\Delta U = U(Z_{u2}) - U(Z_{u1})$, $\Delta \theta = \theta(Z_{T2}) - \theta(Z_{T1})$

4.1 In the unstable case, equations (16) - (17) cannot be solved analytically. Here a numerical iteration has proved to be a good method to obtain the solutions. The procedure is as follows:-

First step: take the neutral case values of U_* and θ_* as the first estimate,

$$U_* = k\Delta U / (\ln Z_{u2}/Z_{u1})$$

$$\theta_* = -k\Delta\theta / (\alpha \ln Z_{T2}/Z_{T1})$$

This is the case for ψ_m and ψ_h with $|L| \rightarrow \infty$. This provides a first estimate of L from,

$$L = - \frac{\bar{\theta}}{g} \frac{U_*^2}{k\theta_*}$$

Second step: substitute this value of L into (10) and (11) (or (14) and (15)), to obtain improved values of U_* and θ_* , and hence an improved value of L .

Third step: substitute the improved value of L into (10) and (11) (or (14) and (15)) again. Repeat this cycle until the successive values of L do not change by more than the required accuracy, e.g.

$$\left| \frac{L_N - L_{N+1}}{L_N} \right| < 0.01$$

In practice it appears that only very few steps (normally not more than 3) are needed to achieve the required accuracy, say, 1%.

4.2 For the stable case, equations (16a) and (16b) can be solved analytically. We have

$$U_* = \left[k \Delta U + \beta \frac{kg}{\theta} (Z_{u2} - Z_{u1}) \frac{\Delta\theta}{\Delta U} \right] / \ln \left(\frac{Z_{u2}}{Z_{u1}} \right) \quad (18)$$

$$\theta_* = \left[k\Delta\theta + \beta \frac{kg}{\theta} (Z_{T2} - Z_{T1}) \left(\frac{\Delta\theta}{\Delta U} \right)^2 \right] / \ln \left(\frac{Z_{T2}}{Z_{T1}} \right) \quad (19)$$

4.3 There are some points which should be noted for the calculation.

a. In the unstable case, fortunately, the iteration procedure always converges.

b. In the stable case, other authors have used different methods to do the calculation, i.e. either an iterative calculation as in the unstable case, or solving (17) as a quadratic equation in L. But the quadratic equation has not a real solution when the determinant of the equation is less than zero. This is the same result as if we solve equation (17) graphically and cannot find the intercept of the straight line $L'=L$ with the curve $F(L) = \psi_n/\psi_m^2$: this occurs when

$$\frac{1}{\beta} \cdot \frac{\theta}{g} \cdot \frac{(\Delta U)^2}{\Delta\theta} \frac{(Z_{T2} - Z_{T1})}{(Z_{u2} - Z_{u1})^2} \leq 1 \quad (20)$$

and the iteration procedure of calculating L and fluxes becomes divergent.

Solving equation (18) and (19) analytically may be the easiest way for the stable case calculation, but this is still limited by condition (20). When (20) happens (normally at low wind speed), from (198), U_* becomes negative; other results, e.g. H, become apparently wrong also.

Condition (20), in fact, is a limit of the validity of the universal functions ϕ_m, ϕ_n given by (6) and (7). Let R_i be the Richardson number, then by definition,

$$\begin{aligned} R_i &= \frac{g}{\theta} \frac{(\partial\theta/\partial Z)}{(\partial U/\partial Z)^2} \\ &\approx \frac{g}{\theta} \frac{\Delta\theta}{(\Delta U)^2} \frac{(Z_{u2} - Z_{u1})^2}{(Z_{T2} - Z_{T1})} \end{aligned} \quad (21)$$

Comparing this with (20) we have

$$R_i \geq \frac{1}{\beta} = 0.2 \quad (22)$$

This is equivalent to condition (20). On the other hand, in the stable case, the turbulent transfer coefficient of momentum

$$\begin{aligned}
 K_m &= U_*^2 / (\partial U / \partial Z) = kZU_* (1 + \beta \frac{Z}{L})^{-1} \\
 &= kZU_*(1 - \beta R_i) \quad (23)
 \end{aligned}$$

where we have used the formula

$$R_i = \frac{Z}{L} \frac{\theta_h}{\theta_m^2} = \frac{Z/L}{1 + \beta Z/L} \quad (24)$$

If $R_i \rightarrow 0.2$, it is implied by (23) that the turbulent transfer is suppressed. Webb (1970) has concluded that the log-linear formulation ((12), (13)) breaks down at about $Z/L = 1$, i.e. $R_i \sim 0.17$, above which a second regime should be used. Carson and Richards (1978) have discussed some other formulations of the similarity functions for the stable condition.

c. Many authors have discussed ways of estimating the roughness length Z_0 . If Z_0 is known, the left-hand side of equation (16a) becomes a wind speed at a single height. Other calculations can be done with the same procedure as above. Berkowicz and Prahm (1981) have proved that the error arising from the uncertainty in determination of Z_0 is smaller than the error resulting from measurements of the wind speed difference. They recommended the use of measurements of wind speed at only one height, with a temperature difference and an independently estimated roughness length Z_0 , to evaluate the fluxes of sensible heat and momentum.

4.4 Calculation of fluxes via the estimation of R_i

As shown in (24), we can relate the Richardson number R_i to the Monin-Obukhov length L as follows

$$R_i = \frac{Z}{L} \frac{\theta_h}{\theta_m^2} \sim \begin{cases} Z/L & \text{(unstable)} \\ 1 + 5 \cdot Z/L & \text{(stable)} \end{cases} \quad (25)$$

(for Dyer and Hick's parameterizations). R_i can be estimated by the finite difference method as shown in (21). Hence, L can be obtained by (25), where Z is assumed to be the geometrical mean height of the layer concerned. If wind and temperature are measured at same height Z_1 and Z_2 , then (21) is simplified,

$$R_i \sim \frac{g}{\theta} \frac{\Delta\theta}{(\Delta U)^2} (Z_2 - Z_1) \quad (26)$$

and $Z = \sqrt{Z_1 \cdot Z_2}$ can be used in (25) for deriving L . Afterwards, H and U_* can be calculated by using (16a) - (16d) as before.

This method is less accurate than the iterative method shown in 4.1 because of a rougher estimation of R_i . But some workers still prefer to use this method since it has produced satisfactory results in most cases and it is easy to use.

5. Comparison with experimental results

The experiments we have chosen below all have high quality wind and temperature profile data. The surface layer heat and momentum fluxes to be compared were either measured directly by use of the eddy correlation method (with sonic anemometer, hot wire/film anemometer, etc.) or, for the sensible heat flux, deduced from the energy balance equation

$$H = R_n - G - LE \quad (27)$$

by measuring net radiation R_n , soil heat flux G and latent heat flux LE .

Over a wide variety of conditions the comparison is found to be satisfactory. The scattering of the data points in the figures is relevant to the limited accuracy of the measurements (in particular, the measurements of G and LE). Moreover, the comparison of atmospheric turbulence data must be carried out on a statistical basis. Even very advanced instruments mounted close together may still give quite different results over a short period. This is seen clearly in the data from the International Turbulence Comparison Experiment (ITCE) (Garratt et al, 1979) where several fluxatrons and a sonic anemometer were mounted a few meters apart and the data over a short period (10 ~ 30 min.) differed by 10 to 50%.

5.1 The International Turbulence Comparison Experiment (ITCE)

The ITCE was held in Australia during October, 1976. An objective of the ITCE micro-meteorological experiments was to provide surface-layer data for a flat, uniform site in order to complement the results of Businger et al (1971). The data include profile data up to 16 m from three masts, four sets of eddy correlation measurements of the vertical fluxes using both sonic anemometry and 'Fluxatron'. Fig. 3 and 4 illustrate the comparison between the calculated and observed values of sensible heat flux and friction velocity respectively, including the relevant statistical parameters. The 1-8 m wind speed gradient and 1.08 - 8 m temperature gradient data have been used in the calculation. The mean sensible heat flux and friction velocity of the data from various eddy correlation techniques are used for comparison. The overall agreement is quite good.

5.2 The Wangara Experiment

The Wangara experiment (Clarke et al, 1971) was held in Australia in 1967, the main aim being to study the evolution of the planetary boundary layer. The unique status of the Wangara experiment has been praised by many authors and over a decade there have been more than twenty papers published on the analysis of the data. Unfortunately the eddy correlation methods were then still under development. There are only six days for which eddy-flux measurements ('Fluxatron', at 10 m) can be used for comparison. Fig. 5 shows the result. The 1-4 m wind and temperature observations have been used in the calculation.

Here, since the wind and temperature were measured at the same heights, it is much easier to do the calculation by using the method mentioned in 4.4. The result is satisfactory.

The difference between the results of the two calculation methods, i.e. the iterative calculation and the calculation by estimating the Richardson number R_i first, is less than 5%.

Hicks (1981) has used the profile method to deduce the sensible heat flux and friction velocity for the whole period of the Wangara experiment and published his results in a tabulated form.

5.3 Cardington experiment (1976-77)

From Spring 1976 to Spring 1977 an experiment was carried out at the Meteorological Research Unit, RAF, Cardington, designed to measure directly the components in the energy budget over a grass surface, and to study their variation over time scales ranging from one hour to several months (Richards, 1979). Wind and temperature profiles were measured on a 16m mast. Surface energy balance data, including net radiation R_n , ground heat flux, G , and latent heat flux, LE , were measured by radiometer (Kew), soil heat flux plates and lysimeter respectively, and reported on an hourly mean basis. The eddy correlation measurements of fluxes are too sparse to be used as a comparison. So the energy balance equation (27) has been used. The result of 70 hours data comparison is shown in Fig. 6.

5.4 Cardington experiment (1983)

In April to May, 1983, an experiment was carried out in RAF Cardington again in nearly the same manner as the 1976 experiment. The principal objective of this experiment was to study the relationship between the surface-layer fluxes, which are difficult to measure for most stations; and easily accessible routine meteorological data. As a result, a modified model for estimating the surface fluxes by use of the so-called 'resistance method' had been developed (Wang, 1984). Two types of radiometer, three soil heat flux plates at different depths, and a lysimeter had been used to measure R_n , G and LE respectively. The sensible heat flux evaluated by using the energy balance equation (27) has been compared with that derived from the 16m wind and temperature profile data. This is shown in Fig. 7. Fig. 8 shows a comparison of friction velocities, in which U_{*p} is calculated by the profile method, U_{*r} is obtained by the resistance method.

The result of calculation by the method described in 4.4 (i.e. estimating R_i first) has been compared with the result of the normal profile method (4.1 - 4.3). The difference is less than 10%.

6. Concluding remarks

The profile method for the estimation of sensible heat flux and friction velocity in the surface layer is found to work well. This method is based on easily available wind and temperature profile measurements and the well defined similarity functions, namely the flux-gradient relationships. For the profile data, only the wind speed measurements at two heights (or one height with an estimation of the roughness length Z_0) and the associated temperature difference measurements are needed.

For the unstable case calculation, the iteration method is shown to be quickly converging and computationally efficient. A rather easy method, i.e. by estimating the Richardson number first and then calculating L and the fluxes, is shown satisfactory in many cases.

Particularly, the profile method works well in the range of $Z/L \sim -1.0$ to 1.0, where the flux-gradient relationships have been well defined. This range of stability covers the cases most frequently experienced in micrometeorological research. In the case of extremely stable conditions, the performance of the profile method in general is poor.

Acknowledgement

The author is very grateful to Dr Carson and Mr Crabtree for their help in preparing this paper.

References

- Benoit, R., 1977, On the integral of the surface layer profile - gradient functions. *J. Appl. Meteorol.*, 16, 859-860.
- Berkowicz, R. and L.P. Prahm, 1981, Evaluation of the profile method for estimation of surface fluxes of momentum and heat. MST LUFT A-54, Riso National Laboratory.
- Businger, J.A. et al, 1971, Flux-profile relationships in the atmospheric surface layer. *J. Atm. Sci.*, 28, 181-189.
- Carson, D.J. and Richards, P.J.R., 1978, Modelling surface turbulent fluxes in stable conditions. *Boundary-layer Meteorol.*, 14, 67-81.
- Clarke, R.H. et al, 1971, The Wangara experiment: Boundary layer data. Technical paper No. 19, Division of Atmospheric Physics, CSIRO, Australia.
- Dyer, A.J., 1974, A review of flux-profile relationships. *Boundary-layer Meteorol.* 7, 363-372.
- Dyer, A.J. and B.B. Hicks, 1970, Flux-gradient relationships in the constant flux layer. *Quart. J.R. Met. Soc.*, 96, 715-721.
- Garratt, J.R. et al, 1979, The International Turbulence Comparison Experiment (Australia, 1976) - Micrometeorological Support data. Technical paper No. 37, Division of Atmospheric Physics, CSIRO, Australia.
- Hicks, B.B., 1976, Wind profile relationships from the "Wangara" experiment, *Quart. J.R. Met. Soc.*, 102, 535-551.
- Hicks, B.B., 1981, An analysis of Wangara Micrometeorology. NOAA Technical Memorandum ERL ARL-104.
- Nickerson, E.C. and V.E. Smiley, 1975, Surface layer and energy budget parameterizations for mesoscale models. *J. Appl. Meteorol.*, 14, 297-300.
- Richards, C.J., 1979, Micrometeorological Characteristics of the 1976 hot spells. *Met. Mag.*, 108, 11-26.
- Wang Jiemin, 1984, A comparison of several methods of assessing the surface energy balance over a grass surface. (Unpublished).
- Webb, E.K., 1970, Profile relationships, the log-linear range and extension to strong stability. *Quart. J.R. Met. Soc.*, 96, 67-90.

List of Figures

- Fig. 1 Similarity functions $\phi_m = \phi_m/K$ and $\phi_h = \phi_h/K$
 $\phi_m(B)$, $\phi_h(B)$ ~ Businger et al's parameterization
 $\phi_m(D)$, $\phi_h(D)$ ~ Dyer and Hicks' parameterization
- Fig. 2 The behaviour of $\psi_m(z)$ under different stabilities. Assume
 $Z_1=Z_0=0.01$ m. $\psi_m(Z) = \frac{k}{u_*} \Delta U = \frac{k}{u_*} U(Z)$.
- Fig. 3 Comparison between measured (H_0) and calculated (H_C) sensible
heat flux for ITCE.
- Mean: $H_C = 169$, $H_0 = 166$
Standard deviation: $\sigma_{HC} = 89$, $\sigma_{HO} = 92$
Correlation: $r = 0.93$
Standard error: $SE = 36$
- Fig. 4 Comparison between measured (U_*0) and calculated (U_*C) friction
velocity for ITCE.
- Mean: $U_*C = 0.34$, $U_*0 = 0.33$
Standard deviation: $\sigma_{U_*C} = 0.08$, $\delta_{U_*0} = 0.10$
Correlation: $r = 0.84$
Standard error: $SE = 0.05$
- Fig. 5 Comparison between measured (H_0) and calculated (H_C) sensible
heat flux for the Wangara experiment
- Mean: $H_C = 127$, $H_0 = 113$
Standard deviation: $\sigma_{HC} = 82$, $\sigma_{HO} = 85$
Correlation: $= 0.91$
Standard error: $SE = 41$
- Fig. 6 Comparison between measured (H_0) and calculated (H_C) sensible
heat flux for the Cardington experiment, 1976.
- Mean: $H_C = 159$, $H_0 = 166$
Standard deviation: $\sigma_{HC} = 81$, $\sigma_{HO} = 64$
Correlation: $= 0.90$
Standard error: $SE = 37$
- Fig. 7 Comparison between measured (H_0) and calculated (H_C) sensible
heat flux for Cardington experiment, 1983.
- Mean: $H_C = 52$, $H_0 = 46$
Standard deviation: $\sigma_{HC} = 76$, $\sigma_{HO} = 80$
Correlation: $= 0.93$
Standard error: $SE = 30$

Fig. 8 A comparison for the friction velocity U_* .

U_{*p} = U_* obtained by profile measurement

U_{*r} = U_* obtained by resistance method

Mean: $U_{*p} = 0.40$, $U_{*r} = 0.38$

Standard deviation: $\sigma_{U_{*p}} = 0.14$, $\sigma_{U_{*r}} = 0.12$

Correlation: $r = 0.95$

Standard error: $SE = 0.05$

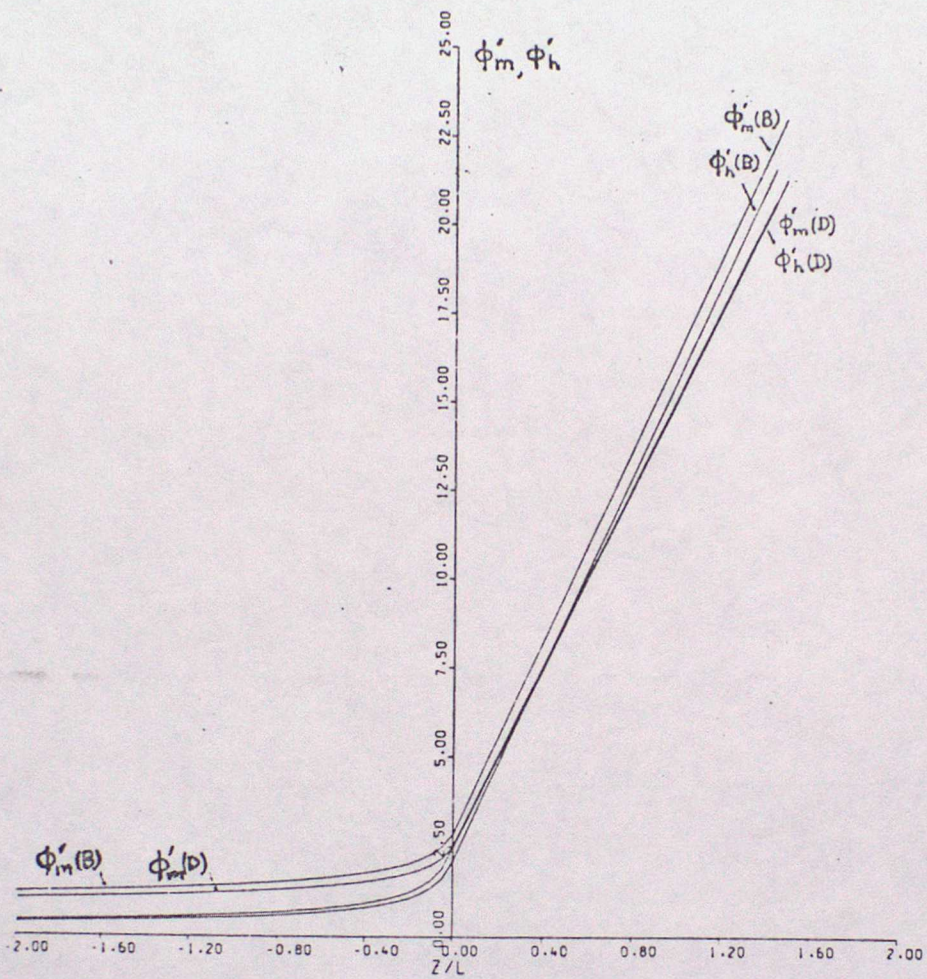


Fig. 1 Similarity functions $\phi'_m = \phi_m/K$ and $\phi'_h = \phi_h/K$
 $\phi_m(B), \phi_h(B)$ - Businger et al's parameterization
 $\phi_m(D), \phi_h(D)$ - Dyer and Hicks' parameterization

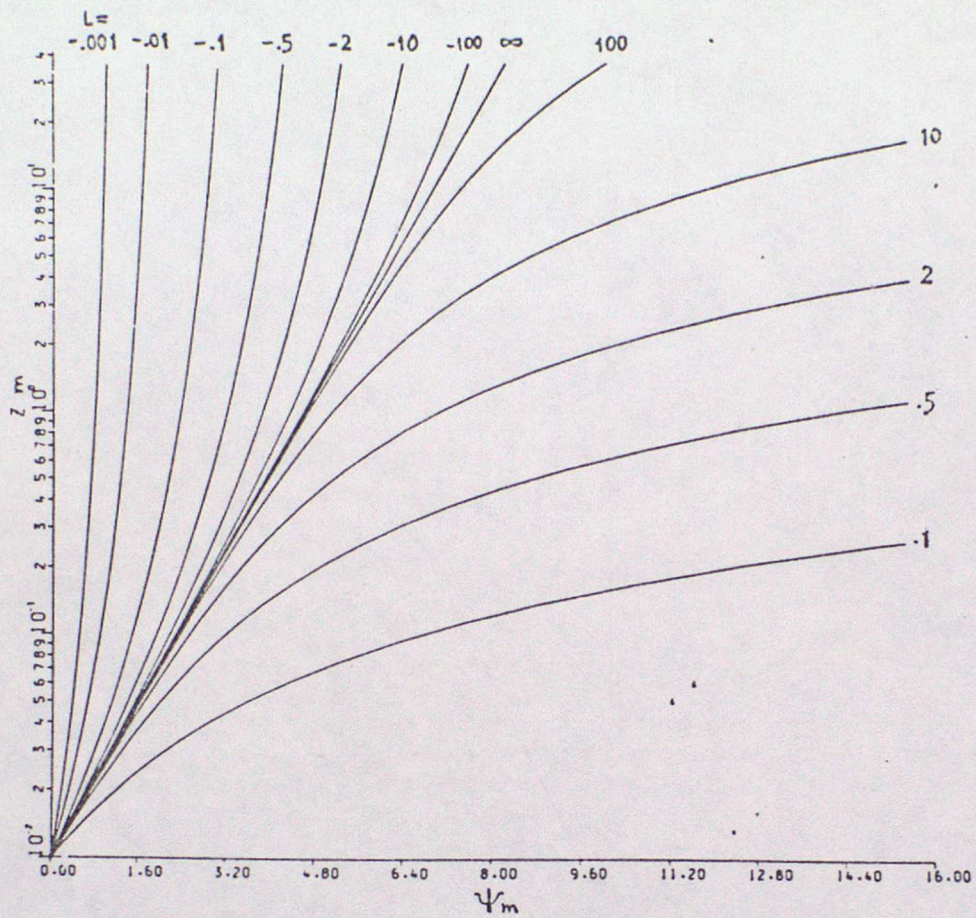


Fig. 2 The behaviour of $\Psi_m(z)$ under different stabilities. Assume $Z_1=Z_0=0.01$ m. $\Psi_m(Z) = \frac{k}{u_*} \Delta U = \frac{k}{u_*} U(Z)$.

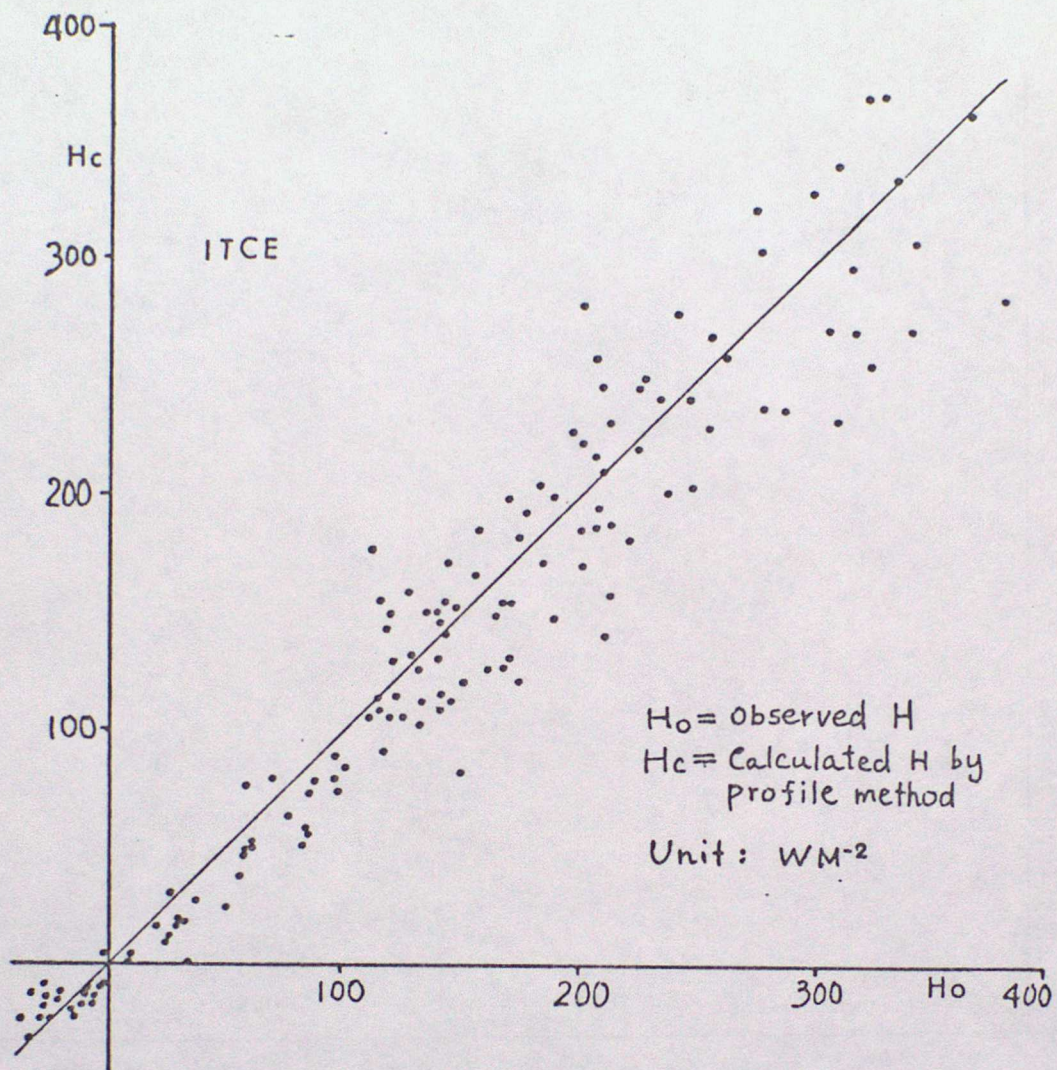


Fig. 3 Comparison between measured (H_O) and calculated (H_C) sensible heat flux for ITCE.

Mean: $H_C = 169$, $H_O = 166$
 Standard deviation: $\sigma_{HC} = 89$, $\sigma_{HO} = 92$
 Correlation: $r = 0.93$
 Standard error: $SE = 36$

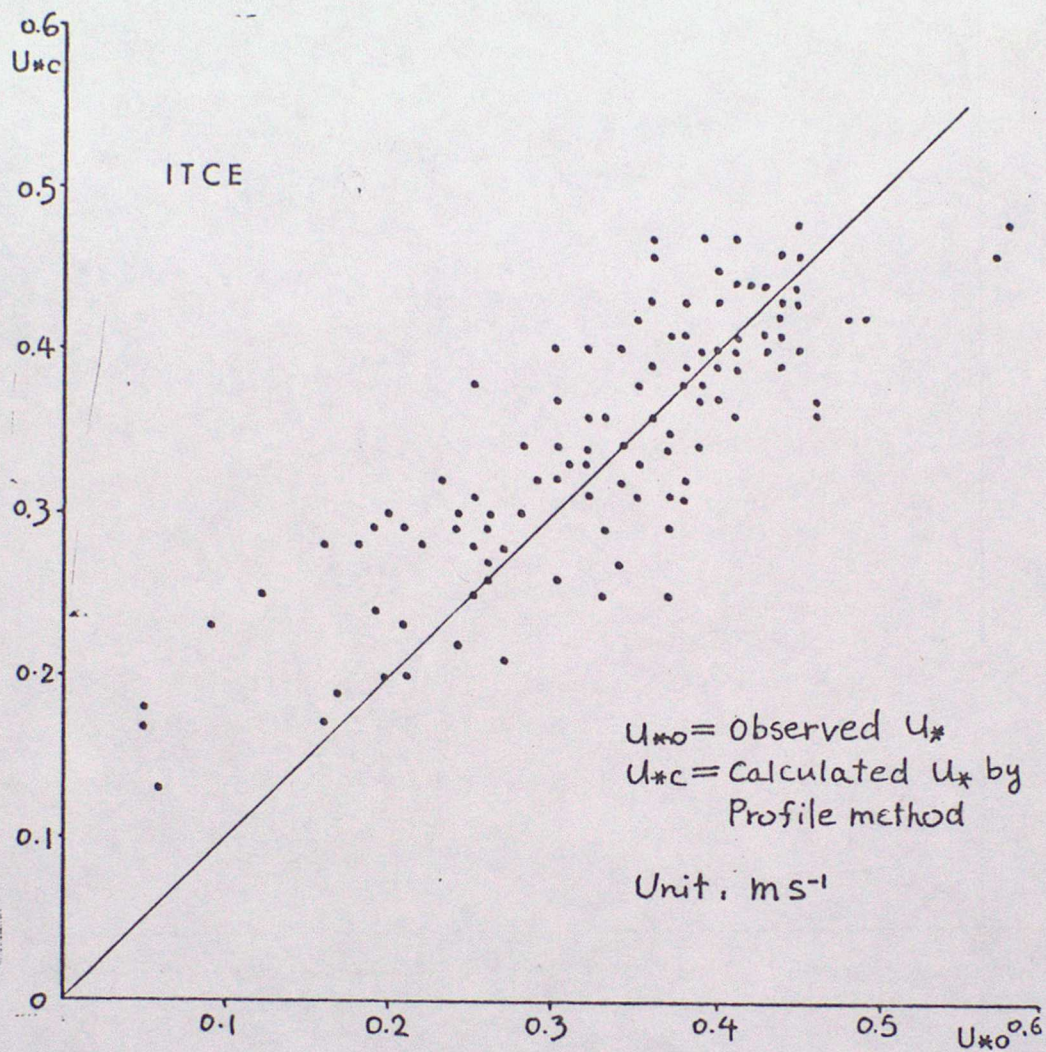


Fig. 4 Comparison between measured (U_{*0}) and calculated (U_{*c}) friction velocity for ITCE.

Mean: $U_{*c} = 0.34$, $U_{*0} = 0.33$
 Standard deviation: $\sigma_{U_{*c}} = 0.08$, $\delta_{U_{*0}} = 0.10$
 Correlation: $r = 0.84$
 Standard error: $SE = 0.05$

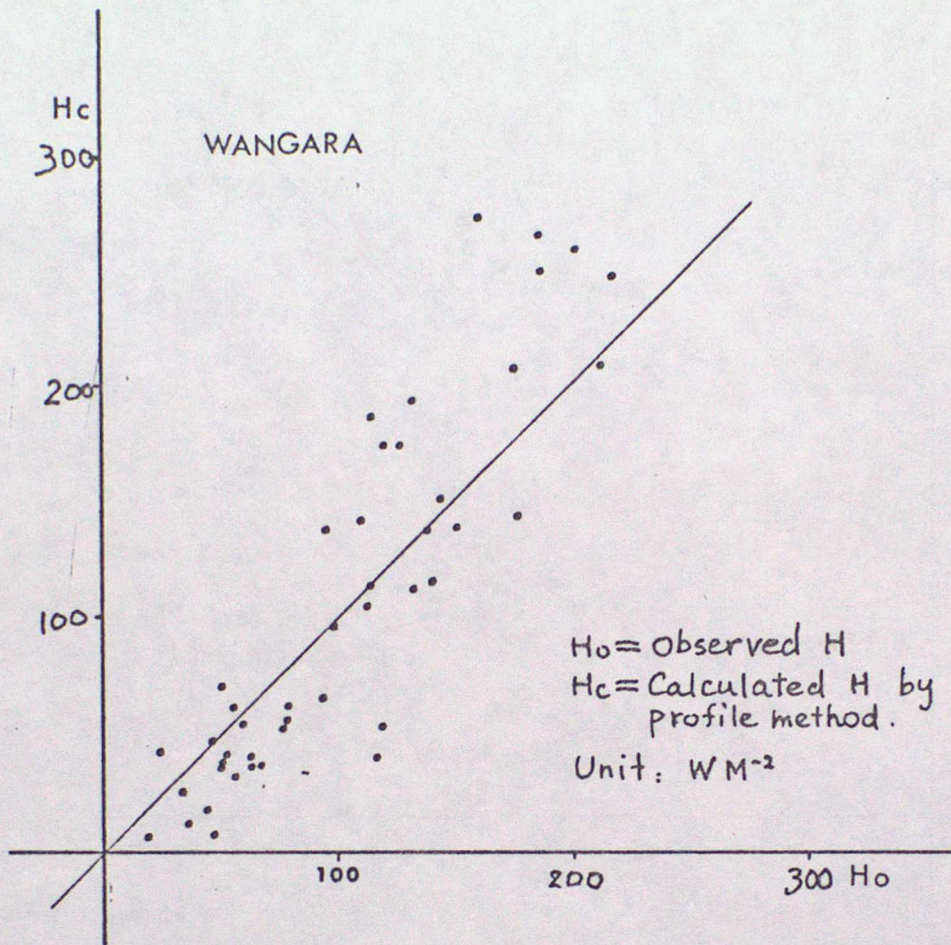


Fig. 5 Comparison between measured (H_o) and calculated (H_c) sensible heat flux for the Wangara experiment

Mean: $H_c = 127$, $H_o = 113$
 Standard deviation: $\sigma_{H_c} = 82$, $\sigma_{H_o} = 85$
 Correlation: $= 0.91$
 Standard error: $SE = 41$

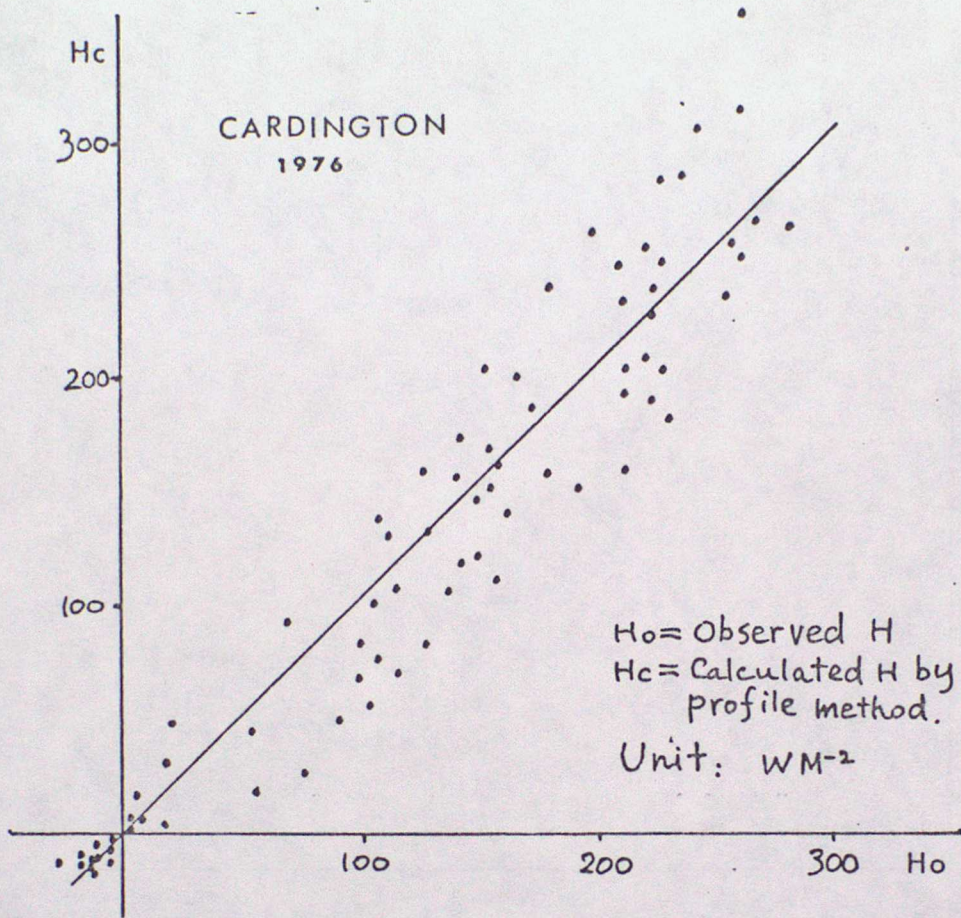


Fig. 6 Comparison between measured (H_o) and calculated (H_c) sensible heat flux for the Cardington experiment, 1976.

Mean: $H_c = 159, H_o = 166$
 Standard deviation: $\sigma_{H_c} = 81, \sigma_{H_o} = 64$
 Correlation: $= 0.90$
 Standard error: $SE = 37$

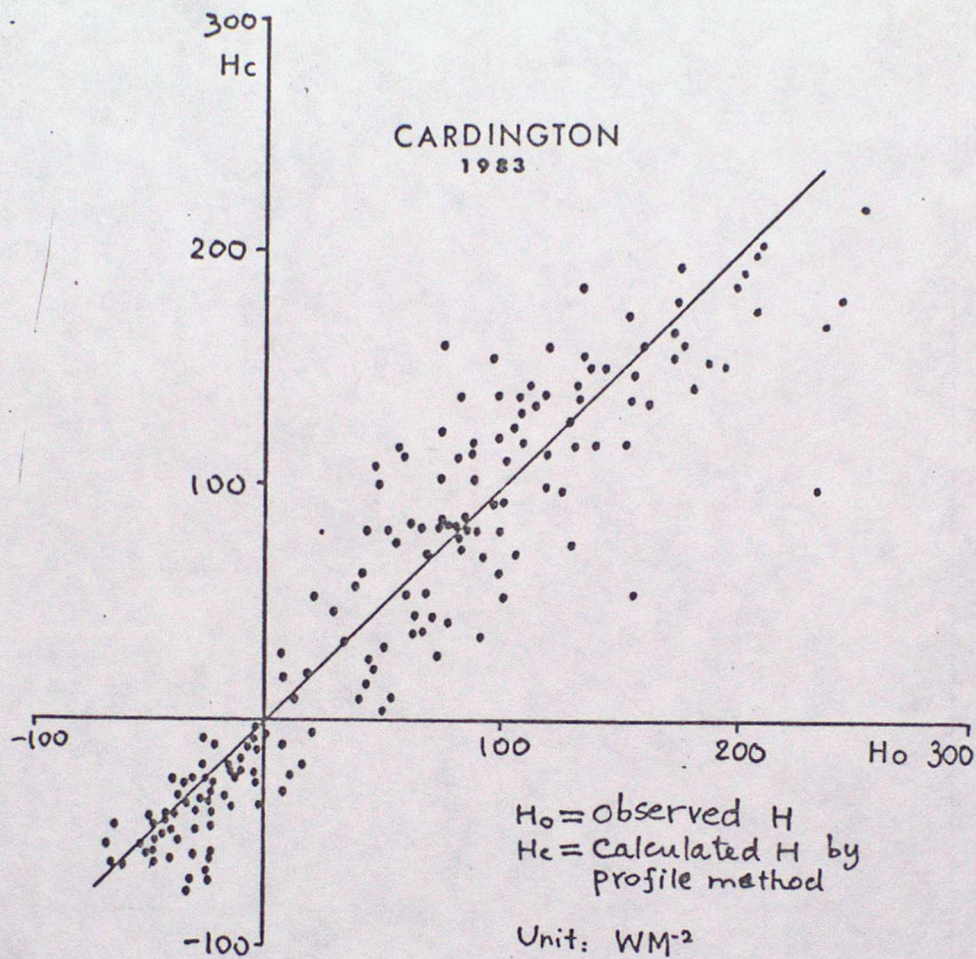


Fig. 7 Comparison between measured (H_0) and calculated (H_c) sensible heat flux for Cardington experiment, 1983.

Mean: $H_c = 52$, $H_0 = 46$
 Standard deviation: $\sigma_{H_c} = 76$, $\sigma_{H_0} = 80$
 Correlation: $= 0.93$
 Standard error: $SE = 30$

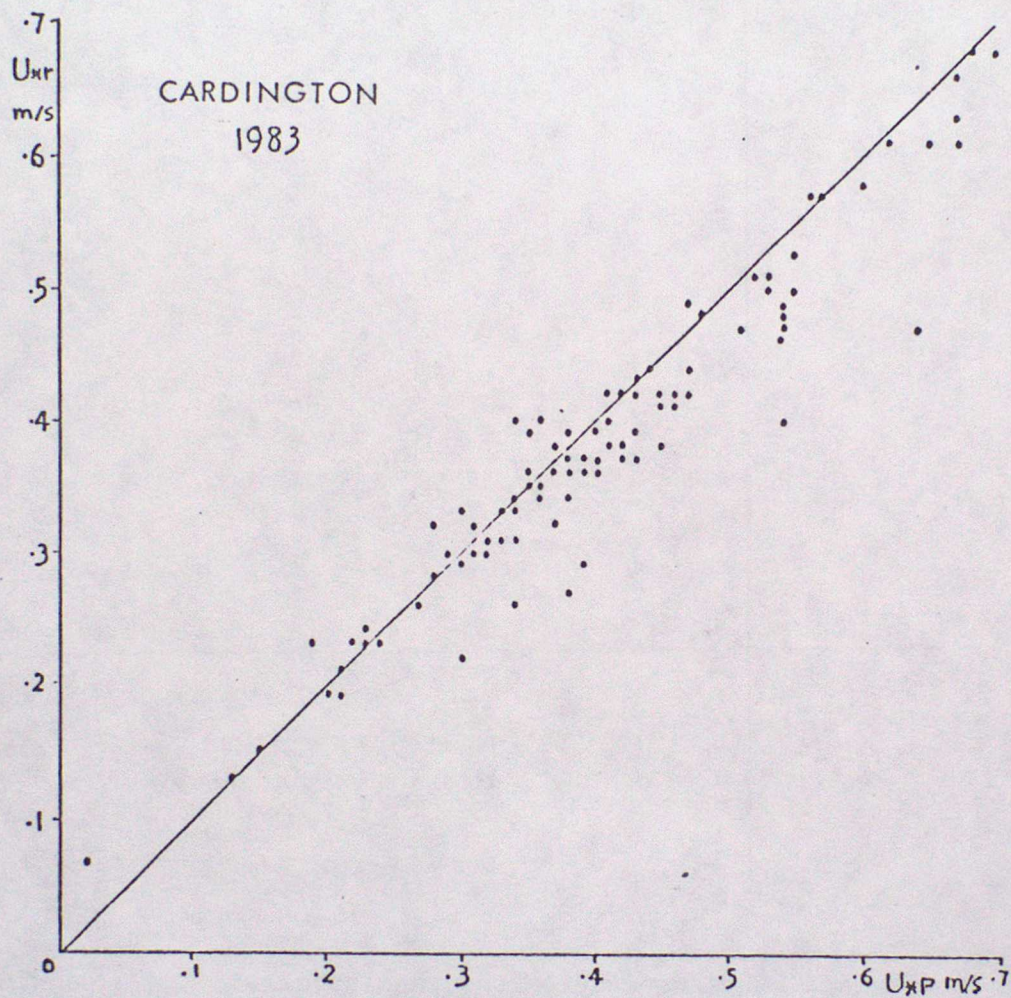


Fig. 8 A comparison for the friction velocity U_* .

U_{*p} = U_* obtained by profile measurement

U_{*r} = U_* obtained by resistance method

Mean: U_{*p} = 0.40, U_{*r} = 0.38

Standard deviation: $\sigma_{U_{*p}}$ = 0.14, $\sigma_{U_{*r}}$ = 0.12

Correlation: r = 0.95

Standard error: SE = 0.05